

Spectrophotometric, Kinetic and Electrochemical Investigations of New Monomeric Hydrazinium Adducts with Ethylenediaminetetraacetatoruthenium(III) Complexes: Catalytic Reduction of Hydrazine to Ammonia in Aqueous Acidic Solution

G. Ramachandraiah

Contribution from the Coordination Chemistry and Homogeneous Catalysis Division, Central Salt & Marine Chemical Research Institute, Bhavnagar-364002, India

Received July 22, 1993*

Abstract: The reaction of hydrazinium ion (N_2H_5^+) with $[\text{Ru}^{\text{III}}(\text{HEDTA})(\text{H}_2\text{O})]$ (EDTA = ethylenediaminetetraacetate) is studied in aqueous solution in the pH range 1.0–4.5 at 25 °C by spectrophotometry and voltammetry. The products of the reaction, $[\text{Ru}^{\text{III}}(\text{HEDTA})(\text{N}_2\text{H}_5)]^+$ and $[\text{Ru}^{\text{III}}(\text{EDTA})(\text{N}_2\text{H}_5)]$, stable at pH < 4.5, are found to be formed with the second-order rate constants 5.63×10^{-3} and $0.576 \text{ M}^{-1} \text{ s}^{-1}$, respectively. The former is also prepared and characterized by physicochemical methods. Reduction of the coordinated hydrazine to 2 equiv of ammonia is observed at $E_{1/2} \sim +0.035 \text{ V}$ vs Ag/AgCl by voltammetry. These complexes are used as electrocatalysts for the reduction of hydrazine to ammonia. The turnover rates of formation of moles of ammonia per mole of catalyst per hour are 18.4 at pH 2.8 and 9.5 at pH 1.9 with 100% Coulombic efficiency, as calculated in constant-potential electrolyses at -0.05 V (Hg) vs SCE. A suitable mechanism for the catalytic reduction of hydrazine to ammonia in acidic media is proposed.

Introduction

The reduction of dinitrogen to ammonia catalyzed by nitrogenase enzyme proceeds via metal-bound diazene and hydrazine intermediates.^{1–4} Although, a large amount of data on nitrogenases^{1–7} including the crystal structures of Mo–Fe⁵ and Fe–protein⁶ units of nitrogenase and particulars on reactivities of coordinated dinitrogen in transition metal complexes^{8–14} are available, the mechanistic and experimental details of the cleavage of the N–N bond in dinitrogen to get ammonia are not yet well understood. Apart from the reports^{15–26} on characterization and

cleavage of the N–N bond^{22–25} on protonation of isolated metal-bound hydrazine complexes in nonaqueous solvents, not much is known about the hydrazine affinity toward metal ions and reduction to ammonia in aqueous solution. However, a few reports^{27,28} are available on catalytic reduction of hydrazine to ammonia in aqueous solution. Schrauzer et al.²⁷ have reported the reduction of hydrazine to ammonia using sodium molybdate–cysteine as catalyst and NaBH_4 as reducing agent with a turnover rate of 4.2 moles of ammonia per mole of catalyst per hour. Later, Hozumi et al.²⁸ reported the catalytic reduction of hydrazine with concomitant evolution of H_2 gas at the Hg cathode (-1.3 V vs SCE) using $[\text{Mo}_2\text{Fe}_4\text{S}_8\text{L}_9]^{3-}$ and $[\text{Fe}_4\text{S}_4\text{L}_4]^{2-}$ (where L = SPh or $\text{SCH}_2\text{CH}_2\text{OH}$) as catalysts. The turnover rates were reported to be less than 10, and the Coulombic efficiency was around 5% at pH 7 and 56% at pH 12. In both cases, neither the nature of the hydrazine species nor the involvement of metal-bound hydrazine undergoing reduction was known. In another report, the oxidation of Cr(II)²⁹ was wrongly attributed to hydrazine reduction; however, this was clarified in a later report³⁰ to be due to oxygen impurity.

The present study, based on the catalytic activity of EDTA complexes of ruthenium,^{31,32} is conducted with a view to understand more about the mechanism of the reduction of the N–N bond in hydrazine to ammonia at a metal center in a protic environment. In this paper, the spectrophotometric, kinetic, and electrochemical investigations on the adducts of hydrazinium ion

- * Abstract published in *Advance ACS Abstracts*, June 15, 1994.
- (1) Burgess, B. K. In *Advances in Nitrogen Fixation Research*; Veegar, C., Newton, W. E., Eds.; Dr. W. Junk/Martinus Nijhoff: Boston, 1984; p 103.
 - (2) Orme-Johnson, W. H. *Annu. Rev. Biophys. Biophys. Chem.* **1985**, *14*, 419.
 - (3) Burgess, B. K. *Chem. Rev.* **1990**, *90*, 1377.
 - (4) Leigh, G. J. *J. Mol. Catal.* **1988**, *47*, 363.
 - (5) Kim, J.; Rees, D. C. *Science* **1992**, *257*, 1667.
 - (6) Georgiadis, M. M.; Komiya, H.; Chakrabarti, P.; Woo, D.; Kornuc, J.; Rees, D. C. *Science* **1992**, *257*, 1653.
 - (7) Wolle, D.; Dean, D. R.; Howard, J. B. *Science* **1992**, *258*, 992.
 - (8) Chatt, J.; Dilworth, J. R.; Richards, R. L. *Chem. Rev.* **1978**, *78*, 589.
 - (9) Hidai, M.; Mizobe, Y. In *Reactions of Coordinated Ligands*, Braterman, P. R., Ed.; Plenum: New York, 1989; Vol. II.
 - (10) Taqui Khan, M. M.; Martell, A. E. *Homogeneous Catalysis by Metal Complexes*; Academic Press: New York, 1974; Vol. I, p 181.
 - (11) Selmann, D. *Angew. Chem., Int. Ed. Engl.* **1974**, *13*, 639.
 - (12) George, T. A.; Tisdale, R. C. *Inorg. Chem.* **1988**, *27*, 2909.
 - (13) Leigh, G. J. *Trans. Met. Chem.* **1986**, *11*, 118.
 - (14) Nishihara, H.; Mori, T.; Tsurita, Y.; Nakano, K.; Saito, T.; Sasaki, Y. *J. Am. Chem. Soc.* **1982**, *104*, 4367 and refs 2–5 in it.
 - (15) Kawano, M.; Hoshino, C.; Matsumoto, K. *Inorg. Chem.* **1992**, *31*, 5158.
 - (16) Vogel, S.; Barth, A.; Huntner, G.; Klein, T.; Zsolnai, L.; Kremer, R. *Angew. Chem., Int. Ed. Engl.* **1991**, *30*, 303.
 - (17) Blum, L.; Williams, I. D.; Schrock, R. R. *J. Am. Chem. Soc.* **1984**, *106*, 8316.
 - (18) Challen, P. R.; Koo, S. M.; Kim, C. G.; Dunham, W. R. Coucouvanis, D. *J. Am. Chem. Soc.* **1990**, *112*, 8606.
 - (19) Rehder, D.; Woitha, C.; Priebsch, W.; Gailus, H. *J. Chem. Soc., Chem. Commun.* **1992**, 364.
 - (20) Tsagkalidis, W.; Woitha, C.; Rehder, D. *Inorg. Chim. Acta.* **1993**, *205*, 239.
 - (21) Dilworth, J. R.; Jobanputra, P.; Miller, J. R.; Parrott, S. *Polyhedron* **1991**, *12*, 513.

- (22) Cai, S.; Schrock, R. R. *Inorg. Chem.* **1991**, *30*, 4105.
- (23) Schrock, R. R.; Glassman, T. E.; Vale, M. G.; Kol, M. *J. Am. Chem. Soc.* **1993**, *115*, 1760.
- (24) Schrock, R. R.; Glassman, T. E.; Vale, M. G. *J. Am. Chem. Soc.* **1991**, *113*, 725.
- (25) Vale, M. G.; Schrock, R. R. *Inorg. Chem.* **1993**, *32*, 2767.
- (26) Frisch, P. D.; Hunt, M. M.; George Kite, W.; McCleverty, J. A.; Rae, A. E.; Seddon, D.; Swann, D.; Williams, J. *J. Chem. Soc., Dalton Trans.* **1979**, 1819.
- (27) Schrauzer, G. N.; Robinson, F. R.; Moorehead, E. L.; Vickrey, T. M. *J. Am. Chem. Soc.* **1976**, *98*, 2815.
- (28) Hozumi, Y.; Imasaka, Y.; Tanaka, K.; Tanaka, T. *Chem. Lett.* **1983**, 897.
- (29) Wells, C. F.; Salam, M. A. *J. Chem. Soc. A* **1968**, 1568.
- (30) Bruhn, S. L.; Bakac, A.; Espenson, J. H. *Inorg. Chem.* **1986**, *25*, 535 and refs. 8 and 9 in it.

with $[\text{Ru}^{\text{III}}(\text{HEDTA})(\text{H}_2\text{O})]$ species are discussed, and the function of these complexes as electrocatalysts for the reduction of hydrazine in acidic media is elucidated.

Experimental Section

Materials and Methods. The complex $\text{K}[\text{Ru}^{\text{III}}(\text{HEDTA})\text{Cl}]\cdot 2\text{H}_2\text{O}$ was prepared from $\text{K}_2[\text{Ru}^{\text{III}}\text{Cl}_5(\text{H}_2\text{O})]$ according to the reported procedure^{33,34} and characterized by UV-vis, IR, potentiometry, and analytical techniques.^{35,36} In aqueous solution, the complex changes to $[\text{Ru}^{\text{III}}(\text{HEDTA})(\text{H}_2\text{O})]$, because of the extraordinary lability of the Ru(III)-Cl bond,^{32c} as observed from kinetic and spectrophotometric data,³⁷ and hence $\text{K}[\text{Ru}^{\text{III}}(\text{HEDTA})\text{Cl}]\cdot 2(\text{H}_2\text{O})$ was used as a source for the aquo complex in the present studies. Hydrazinesulfate ($\text{N}_2\text{H}_5\text{HSO}_4$) from BDH Chemicals was used. Stock solutions of hydrazinesulfate were prepared, standardized with potassium iodate,³⁸ and used to prepare experimental solutions. Hydrazine (N_2H_4), in stock as well as in experimental solutions in the pH range 1.0–4.5, would really mean hydrazinium (N_2H_5^+) ion, as discussed later. All the chemicals used were of analytical grade. Experimental solutions were prepared in 0.1 M sodium acetate as supporting electrolyte, and pH was adjusted to the desired value within ± 0.01 pH using H_2SO_4 solution. Argon gas was employed to flush out the dissolved oxygen in all the solutions.

The UV-vis spectral measurements were carried out in a 10-mm quartz cuvette by monitoring the decrease in absorbance of $[\text{Ru}^{\text{III}}(\text{HEDTA})(\text{H}_2\text{O})]$ at 360 nm using a Shimadzu UV-vis NIR scanning spectrophotometer UV-3101 PC. The kinetic data were obtained using a Hi-Tech Stopped-Flow Spectrophotometer SF-51 coupled to an Apple data processor. The cell compartment was thermostated to 25 ± 0.01 °C. In these studies, the complex concentration was kept constant (3 mM) and the hydrazine concentration was maintained at at least 10-fold excess. The pseudo-first-order kinetic data were analyzed with the help of a data acquisition program for at least 2–3 half-lives of the reaction.

Sampled DC, differential pulse polarography (dpp), and cyclic voltammetry (CV) experiments were conducted using Princeton Applied Research models: 174A Polarographic Analyzer, 175 Universal Programmer, and a Houston Instruments X-Y recorder. A weighed quantity of the complex and a measured volume of hydrazinesulfate from the stock solution were added to a 10-mL solution of the electrolyte in a single-compartment cell. A weighed quantity of hydrazinesulfate was further added when the molar concentration of hydrazine needed to be raised. The pH of the experimental solution containing complex (1 mM) and hydrazine (1 or 60 mM) in 0.1 N H_2SO_4 was varied to examine the pH effect on diffusion current by adding appropriate amounts of sodium acetate (4 M) solution. A Pt wire auxiliary and a KCl saturated Ag/AgCl reference electrodes fitted in a PAR 303 assembly were employed with either a dropping (3.85 mg s^{-1}) or a hanging mercury drop (0.021 cm^2) as working electrode. The i - E plots in sampled DC, dpp, and CV, experiments were recorded from +0.2 to -0.5 at the following sweep rates: 10, 5, and 20–500 mV s^{-1} , respectively. The electrochemical cell was thermostated (25 °C or to the desired value) within ± 0.1 °C.

The techniques developed by Meites³⁹ were adopted for measuring polarographic wave heights and half wave potentials. The diffusion of the voltammetric currents was checked by the linear dependence of i_d on the concentration of complex (0.1–3.0 mM) and capillary characteristics ($m^{2/3}l^{1/6}$) in polarography and of i_p on $v^{1/2}$ (v = scan speed) in CV measurements. The semilog plot and the measure of $E_{1/4} - E_{3/4}$ (56.4/n

mV) in polarography and i_{pa}/i_{pc} and $E_{p/2} - E_p$ (56.5/n mV) in CV were taken as the criteria for electrochemical reversibility.

Controlled-potential electrolyses were carried out using PAR models 173 galvanostat and 179 digital coulometer in a three-compartmental cell. The reference electrode, SCE, was brought into the actual reaction compartment via a vycor-tipped glass tube filled with buffer solution. The auxiliary Pt mesh electrode was separated from the main compartment by a fine (G4) glass frit. The main compartment contained mercury (1-in. convex surface diameter) with a glass agitator just above the mercury surface. In a typical experiment, a 30-mL solution of 0.2 M sodium acetate at desired pH contained 30 μmol of complex and 2.4 mmol of hydrazinesulfate. The solution was potentiostated at -0.05 V with constant stirring under argon. The electrolysis was continued for 6 h, and the quantity of ammonia produced was estimated at half-hour intervals by using an Orion 940 ion analyzer equipped with an ammonia-sensing electrode. Samples for this were prepared by adding 1 mL of the experimental solution to 2 mL of 2 M NaOH solution diluted to 50 mL. These results were checked by the dpp method.⁴⁰

EPR measurements were done on a Bruker ESP-300 \times band instrument with a 100-kHz field modulation using DPPH as a field marker ($g = 2.0036$). EPR spectra for $[\text{Ru}^{\text{III}}(\text{HEDTA})(\text{H}_2\text{O})]$ (6 mM) before and after adding hydrazinesulfate (30 mM) at pH 3 were recorded at 25 °C using a B-ER400 Z-EZ cell.

Preparation of $[\text{Ru}^{\text{III}}(\text{HEDTA})(\text{N}_2\text{H}_5)]\text{HSO}_4$: Hydrazinesulfate (0.055 g, 0.42 mmol) was added to a solution of $\text{K}[\text{Ru}^{\text{III}}(\text{HEDTA})\text{Cl}]\cdot 2\text{H}_2\text{O}$ (0.20 g, 0.4 mmol) at its own pH (~ 2.8) in a minimum volume of water. The solution was stirred for 40 min at room temperature under a nitrogen atmosphere. The hydrazinium complex was then precipitated with excess acetone, filtered off, washed with a 1:9 water-acetone mixture, and then dried under vacuum. Anal. Calcd: C, 23.05; N, 10.77; H, 3.65. Found: C, 23.56; N, 10.52; H, 3.81. IR 1727 cm^{-1} for COOH, 1630 cm^{-1} for bound COO⁻, 3229 cm^{-1} for N-H stretching, 1415 and 1122 cm^{-1} for N-H deformations. The complex showed no absorption band at 360 nm.

Results and Discussion

I. Investigation of Hydrazinium Complexes in Solution: Spectrophotometry. Initial experiments were carried out to investigate the reactivity of hydrazine with $[\text{Ru}^{\text{III}}(\text{HEDTA})(\text{H}_2\text{O})]$ over the pH range 1–9. At $\text{pH} \leq 4.5$, the addition of hydrazine to the complex solution did not show any color change or give a new peak in the visible region, except a significant reduction in the absorbance of the shoulder at 360 nm, which is a characteristic feature for the aquo complex.^{41,42} However, at $\text{pH} > 4.5$, the light-yellow color of the complex solution rapidly changed, first to pink and then to orange yellow or yellowish green, depending on the solution pH. In this pH range, a weak band at 520 nm developed gradually and diminished later during the course of reaction; a new band at 420 nm developed above pH 8 and remained constant. This spectral behavior above pH 4.5 is indicative of formation and decomposition⁴³ of hydrazine complexes, and hence the present study is confined to the pH range < 4.5 .

The observed change in the absorption spectra of $[\text{Ru}^{\text{III}}(\text{HEDTA})(\text{H}_2\text{O})]$ at $\text{pH} = 3$ with the addition of hydrazine is depicted in Figure 1A. The disappearance of the shoulder at 360 nm is indicated as the coordination of hydrazine. Similar spectral features were also reported for an N-donated isonicotinamide and pyrazine derivatives of $[\text{Ru}^{\text{III}}(\text{HEDTA})(\text{H}_2\text{O})]$.⁴² A plot of

(31) (a) Taqui Khan, M. M.; Siddiqui, M. R. H.; Hussain, A.; Moiz, M. A. *Inorg. Chem.* **1986**, *25*, 2765. (b) Taqui Khan, M. M.; Shukla, R. S.; Rao, A. P. *Inorg. Chem.* **1989**, *28*, 452. (c) Taqui Khan, M. M.; Chatterjee, D.; Merchant, R. R.; Paul, P.; Abdi, S. H. R.; Srinivas, D.; Moiz, M. A.; Bhadbhade, M. M.; Venkatasubramanian, K. *Inorg. Chem.* **1992**, *31*, 2711. (d) Taqui Khan, M. M.; Bhardwaz, R. C.; Bhardwaz, C. *Angew. Chem., Int. Ed. Engl.* **1988**, *27*, 927. (e) Taqui Khan, M. M.; Halligudi, S. B.; Shukla, S. *Angew. Chem., Int. Ed. Engl.* **1988**, *27*, 734.

(32) Rhodes, M. R.; Barley, M. H.; Meyer, T. J. *Inorg. Chem.* **1991**, *30*, 629.

(33) Diamantis, A. A.; Dubrawski, J. V. *Inorg. Chem.* **1981**, *20*, 1142.

(34) Mercer, E. E.; Buckley, R. R. *Inorg. Chem.* **1965**, *4*, 1692.

(35) Taqui Khan, M. M.; Kumar, A.; Shirin, Z. *J. Chem. Res.* **1986**, *5*, 1003.

(36) Taqui Khan, M. M.; Hussain, A.; Ramachandraiah, G.; Moiz, M. A. *Inorg. Chem.* **1986**, *25*, 3023.

(37) Bajaj, H. C.; van Eldik, R. *Inorg. Chem.* **1988**, *27*, 4052.

(38) Vogel, A. I., Ed. *Text Book of Quantitative Inorganic Analysis*; Longman Group Ltd.: London, 1978; p 390.

(39) Meites, L. *Polarographic Techniques*, 2nd ed.; Interscience: New York, 1967.

(40) The experimental solution (0.1 mL) was added to 10 mL of a 1:1 acetic acid-sodium acetate buffer (0.4 M, pH 4) and formaldehyde (37%), mixture and its dpp was run from -0.6 to -1.1 V. The peak current at -0.9 V for the reduction of hexamethylenetetramine resulted by the reaction of ammonia in the experimental solution with the formaldehyde was measured and compared with that of a standard. For other experimental details see: Application Brief A-3 (Ammonia), Princeton Applied Research Corp., USA, 1976.

(41) Matsubara, T.; Creutz, C. *Inorg. Chem.* **1979**, *18*, 1956.

(42) Taqui Khan, M. M.; Moiz, M. A.; Hussain, A. *J. Coord. Chem.* **1991**, *23*, 245.

(43) (a) The decomposition/oxidation of hydrazine by transition metals or their complexes is reported. See: Minato, H.; Mechan, E. J.; Kolthoff, I. M.; Auerbach, C. *J. Am. Chem. Soc.* **1959**, *81*, 6168. Higginson, W. C. E.; Wright, P. *J. Chem. Soc.* **1953**, 1380; **1955**, 1551. (b) The decomposition of hydrazinium complexes of $[\text{Ru}^{\text{III}}(\text{HEDTA})(\text{H}_2\text{O})]$ was observed above pH 4.5.

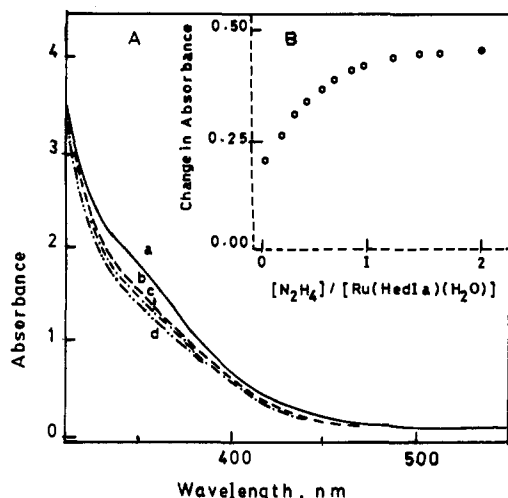


Figure 1. (A) Absorption spectra of $[\text{Ru}^{\text{III}}(\text{HEDTA})(\text{H}_2\text{O})]$, 2 mM, immediately after the addition of the following concentrations of hydrazine ($10^3[\text{N}_2\text{H}_4]$): (a) 0 M; (b) 0.5 M; (c) 1 M; (d) 2.5 M pH 3. (B) Plot of the change in absorbance (ΔA) at 360 nm vs $[\text{N}_2\text{H}_4]/\{[\text{Ru}^{\text{III}}(\text{HEDTA})(\text{H}_2\text{O})]\}$.

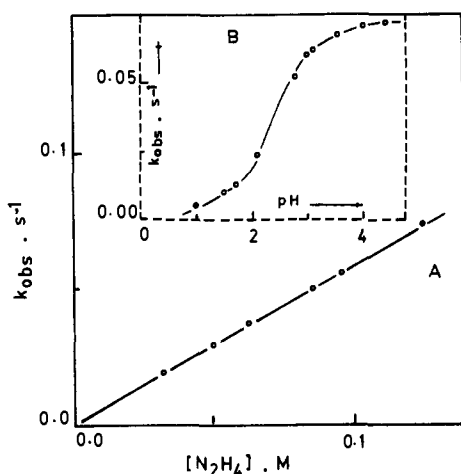
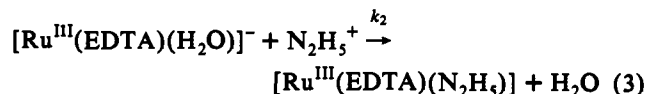
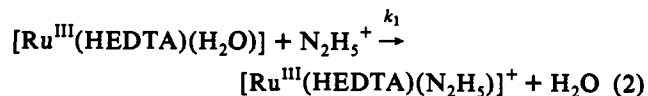
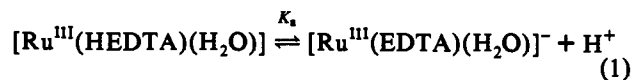


Figure 2. (A) Dependence of k_{obs} on hydrazine concentration $[\text{Ru}^{\text{III}}(\text{HEDTA})(\text{H}_2\text{O})]$, 3 mM, pH 4.4. (B) Plot of k_{obs} vs pH: $[\text{Ru}^{\text{III}}(\text{HEDTA})(\text{H}_2\text{O})]$, 3 mM; $[\text{N}_2\text{H}_4]$, 0.125 M.

absorbance change (ΔA) versus $[\text{hydrazine}]/[\text{Ru}^{\text{III}}(\text{HEDTA})(\text{H}_2\text{O})]$, shown in Figure 1B, suggests the stoichiometry of the reaction to be 1:1.

The observed pseudo-first-order rate constant, k_{obs} , showed a linear dependence on the concentration of hydrazine. The plot of k_{obs} vs $[\text{hydrazine}]$ (Figure 2 A) shows a negligible intercept, indicating the completion of the reaction. The rate constant (k_{obs}) was pH dependent with a maximum value between pH 4 and 4.5 (as shown in Figure 2B), and the inflection seen at pH ~ 2.4 is in close agreement with that of other substitution reactions.^{37,41} The value of the inflection point observed here is comparable to $\text{p}K_a$ (2.37),⁴¹ corresponding to the deprotonation of the free carboxylic acid group of HEDTA. Hydrazine, on the other hand, can exist in two protonated forms, viz. $\text{N}_2\text{H}_6^{2+}$ and N_2H_5^+ in aqueous solution⁴⁴ with acid dissociation constants 11 and 1.02×10^{-8} ,⁴⁵ respectively. Thus, N_2H_5^+ is the most likely species to take part in the reaction under the present experimental conditions. The pH dependence of k_{obs} in Figure 2B is suggested to be due to following the reactions in solution.



From the above reactions, k_{obs} can be expressed as

$$k_{\text{obs}} = \{k_1[\text{H}^+] + k_2K_a\{[\text{N}_2\text{H}_5^+]\}\}/\{[\text{H}^+] + K_a\} \quad (4)$$

From a plot of $k_{\text{obs}}\{[\text{H}^+] + K_a\}/[\text{N}_2\text{H}_5^+]$ vs $[\text{H}^+]$, the second-order rate constants are evaluated to be $k_1 = 5.63 \times 10^{-3} \text{ M}^{-1} \text{ s}^{-1}$ and $k_2 = 0.576 \text{ M}^{-1} \text{ s}^{-1}$. A smaller value of k_1 as compared to k_2 reflects the lower reactivity of $[\text{Ru}^{\text{III}}(\text{HEDTA})(\text{H}_2\text{O})]$ with respect to $[\text{Ru}^{\text{III}}(\text{EDTA})(\text{H}_2\text{O})]^-$.⁴¹

Sampled DC. The polarographic behavior of a solution of $[\text{Ru}^{\text{III}}(\text{HEDTA})(\text{H}_2\text{O})]$ (1 mM) at pH 3 in the absence and presence of hydrazine (0.1–100 mM) is shown in Figure 3A. In the absence of hydrazine, the complex exhibited a well-defined cathodic wave Figure 3A (a) (I , 1.27; $E_{1/4} - E_{3/4}$, 79 mV) at $E_{1/2} = -0.135 \text{ V}$ assigned to $\text{Ru}(\text{III}) \rightarrow \text{Ru}(\text{II})$ reduction.⁴⁶ Its position and height were not changed conspicuously with the change in pH. The wave analysis indicated that the electrode reaction is diffusion controlled and nearly reversible. However, the wave height increased initially with the addition of hydrazine (0.1–1.0 mM) and leveled off later (1–5 mM) because of the development of a new reduction wave overlapping with the original wave. As a result of this, the $E_{1/2}$ appeared to be shifted anodically with an increase in $E_{1/4} - E_{3/4}$ value. These observations are attributed to the rapid formation of hydrazinium complexes and their direct involvement in electrochemical processes. A plot of enhanced current at -0.31 V vs $[\text{hydrazine}]/[\text{Ru}^{\text{III}}(\text{HEDTA})(\text{H}_2\text{O})]$ (Figure 3B) has further confirmed the formation of monomeric hydrazinium adducts as suggested by reactions 2 and 3. The height of this resultant wave ($E_{1/2} \sim -0.087 \text{ V}$; $E_{1/4} - E_{3/4} \sim 120 \text{ mV}$; $I \sim 3$) at $[\text{hydrazine}]/[\text{Ru}^{\text{III}}(\text{HEDTA})(\text{H}_2\text{O})] \geq 1$ is diffusion controlled and proportional to complex concentration (Figure 3C (a)). But, at $[\text{hydrazine}]/[\text{Ru}^{\text{III}}(\text{HEDTA})(\text{H}_2\text{O})] \leq 1$, the increment in wave height was nonlinear. It was observed that the enhanced current was 80% more at $[\text{hydrazine}]/[\text{Ru}^{\text{III}}(\text{HEDTA})(\text{H}_2\text{O})] = 0.25$ and 5% more at $[\text{hydrazine}]/[\text{Ru}^{\text{III}}(\text{HEDTA})(\text{H}_2\text{O})] = 0.75$ than the expected rise, due to the participation of the hydrazinium complex formed at that composition. The reason for this additional (catalytic) current will be discussed in a later part of this paper.

With the increase in concentration of hydrazine above 5 mM, the new wave and the initial wave were clearly seen as two independent steps: step 1 (the new or multielectron wave) and step 2 (at potentials near to the initial $\text{Ru}(\text{III}) \rightarrow \text{Ru}(\text{II})$ wave), as those in Figure 3A (d). Both the waves were diffusion controlled, and their wave heights were proportional to the complex concentration (Figure 3C (b,c)). The log plots of the waves are linear with slopes 0.027 (step 1) and 0.061 (step 2), showing two- and one-electron reductions, respectively. The $E_{1/2}$ of step 1 ($I \approx 0.63$; $E_{1/4} - E_{3/4} \approx 24 \text{ mV}$) was anodically shifted with the increase in hydrazine concentration (slope of the plot $E_{1/2}$ vs $\log [\text{hydrazine}]$ is 0.071), suggesting much more effective coordination of hydrazinium ion to the metal in the reduced complex. The $E_{1/2}$ of step 2 ($I \approx 1.35$; $E_{1/4} - E_{3/4} \approx 55 \text{ mV}$) at -0.140 V was not affected by the concentration of hydrazine.

(44) Latimer, W. M. *The Oxidation States of the Elements and their Potentials in Aqueous Solutions* 2nd ed.; Prentice Hall, Inc: New York, 1952; p 99.

(45) Bhargava, A. P.; Swaroop, R.; Gupta, Y. K. *J. Chem. Soc.* 1970, 2183.

(46) Shimzu, K.; Matsubara, T.; Sato, G. P. *Bull. Chem. Soc. Jpn.* 1974, 47, 1651.

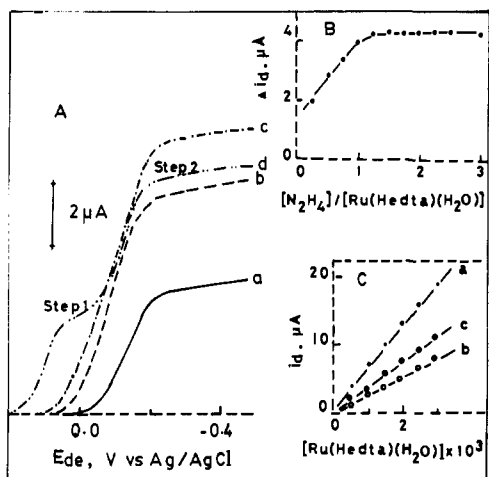


Figure 3. (A) Sampled DC polarograms of $[\text{Ru}^{\text{III}}(\text{HEDTA})(\text{H}_2\text{O})]$, 1 mM (pH 3), in the presence of the following concentrations of hydrazine ($10^3[\text{N}_2\text{H}_4]$): (a) 0 M; (b) 0.5 M; (c) 2.5 M; (d) 60 M. (B) Plot of enhanced diffusion current (Δi_d) at -0.31 V vs $[\text{N}_2\text{H}_4]/[\text{Ru}^{\text{III}}(\text{HEDTA})(\text{H}_2\text{O})]$. (C) Linear dependence of diffusion current (i_d) on $[\text{Ru}^{\text{III}}(\text{HEDTA})(\text{H}_2\text{O})]$ at pH 3 (a) for the composite wave observed in the presence of 3 mM N_2H_4 and (b) for step 1 (c) for step 2 observed in the presence of 60 mM N_2H_4 .

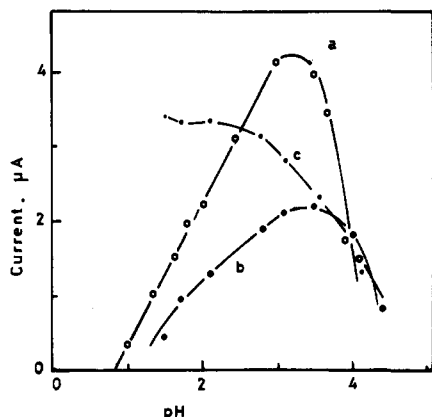


Figure 4. Effect of pH on (a) enhanced current (Δi_d) at -0.31 V in the presence of hydrazine (1 mM) and on the wave heights of (b) step 1 and (c) step 2 in the presence of hydrazine (60 mM). $[\text{Ru}^{\text{III}}(\text{HEDTA})(\text{H}_2\text{O})]$ in all cases was kept at 1 mM.

The heights of polarograms in Figure 3A (c,d) showed a small dependence on the ionic strength of the solution. The overall enhanced current at -0.31 V was reduced by 8% or 20% when Na_2SO_4 (0.5 M) or $(\text{NH}_4)_2\text{SO}_4$ (0.5 M) was added to the solution. The polarographic changes (Figure 3A) were not seen when millimolar concentrations of acetonitrile⁴¹ or thiourea³⁷ were injected into the experimental solution, which indicates the binding of hydrazinium ion to Ru(III) at the sixth labile position.^{37,41} The wave heights, however, enhanced with increased temperature of the solution. The overall diffusion current at -0.31 V became threefold at 50°C to that of the polarogram in Figure 3A (a); this rise was more than the usual 2% rise per degree.³⁹

The effects of hydrogen ion concentration on the enhanced current of the composite wave and the heights of steps 1 and 2 are shown in Figure 4. The lowering of current between pH 2.8 and 1.0 may be due to the decreased rate of formation of the hydrazinium complex with $[\text{Ru}^{\text{III}}(\text{HEDTA})(\text{H}_2\text{O})]$. The reduction in current above pH 3.6 may be accounted for by the shift in quasi-reversible behavior of the Ru(III)/Ru(II) couple to irreversible. The transformation of $[\text{Ru}^{\text{III}}(\text{EDTA})(\text{H}_2\text{O})]^-$ to $[\text{Ru}^{\text{III}}(\text{EDTA})(\text{OH})]^{2-}$ at higher pH was reported earlier.³⁶

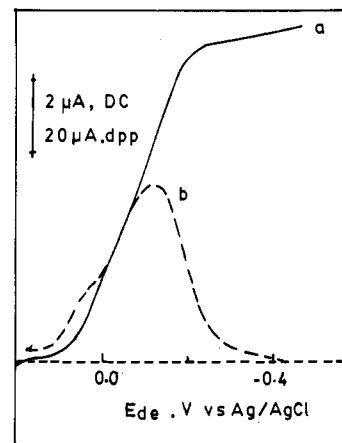


Figure 5. (a) Sampled DC and (b) dpp of $[\text{Ru}^{\text{III}}(\text{HEDTA})(\text{N}_2\text{H}_5)]\text{HSO}_4$ (1 mM) at pH 3.

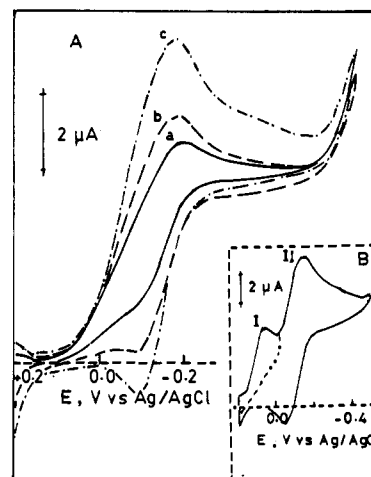


Figure 6. (A) CV responses of $[\text{Ru}^{\text{III}}(\text{HEDTA})(\text{H}_2\text{O})]$ (1 mM) in the presence of hydrazine (1 mM) at scan speeds (a) 0.02, (b) 0.05, (c) 0.10 V s^{-1} . (B) CV of $[\text{Ru}^{\text{III}}(\text{HEDTA})(\text{H}_2\text{O})]$ (1 mM) in the presence of hydrazine (60 mM) at scan speed 0.10 V s^{-1} . pH in all cases was maintained at 3.

The solution of $[\text{Ru}^{\text{III}}(\text{HEDTA})(\text{H}_2\text{O})]$ at pH 3 in an ESR experiment exhibited a paramagnetic signal with $g_{\text{iso}} = 2.057$ before and after the addition of excess hydrazine. Further, it is concluded that the enhanced current shown in Figure 3A is not due to the reduction of oxidized products of $[\text{Ru}^{\text{III}}(\text{HEDTA})(\text{H}_2\text{O})]$ by hydrazine at the electrode but as a result of reduction of the hydrazinium complexes $[\text{Ru}^{\text{III}}(\text{HEDTA})(\text{N}_2\text{H}_5)]^+$ and $[\text{Ru}^{\text{III}}(\text{EDTA})(\text{N}_2\text{H}_5)]$.

The polarographic (sampled DC and dpp) results of $[\text{Ru}^{\text{III}}(\text{HEDTA})(\text{N}_2\text{H}_5)]\text{HSO}_4$ at pH 3 are shown in Figure 5. The reduction steps 1 and 2 as seen in Figure 3A (d) were not well resolved in sampled DC (Figure 5a), but they appeared as separate peaks ($\approx E_{1/2}$) at $+0.035$ and -0.123 V in dpp (Figure 5b).

Cyclic Voltammetry. The complex $[\text{Ru}^{\text{III}}(\text{HEDTA})(\text{H}_2\text{O})]$ in the absence of hydrazine showed a cathodic peak at -0.181 V and an anodic peak at -0.102 V, corresponding to the Ru(III)/Ru(II) redox couple. The peak currents were proportional to the square root of scan speed, while the ratio of anodic to cathodic peak currents was close to unity. The peak to peak separation (ΔE_p) was ~ 80 mV, and $E_{p/2} - E_p \sim 63$ mV. The CV features are consistent with a quasi-reversible, diffusion-controlled electrode process.

Representative cyclic voltammograms at three scan speeds after the addition of hydrazine (≤ 5 mM) are shown in Figure 6A. The cathodic peak grew initially with the hydrazine concentration leveling off as $[\text{hydrazine}]/[\text{Ru}^{\text{III}}(\text{HEDTA})(\text{H}_2\text{O})]$ approached

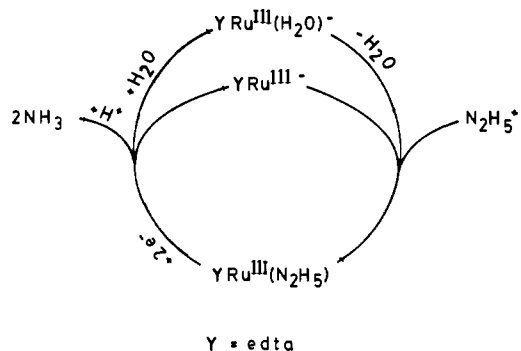
unity. The peak current at the saturation limit (at scan speeds $\geq 100 \text{ mV s}^{-1}$) fulfilled the criterion for a diffusion-controlled process, but at lower speeds it was greater than the expected value. The anodic peak intensity, on the other hand, decreased at higher scan speeds ($\geq 100 \text{ mV s}^{-1}$), tending to disappear at lower speeds. These changes can be attributed to the reduction of the hydrazinium complex to form an intermediate Ru(II) complex (as proposed in the latter part of this paper) which undergoes oxidation in subsequent chemical reactions. The cathodic peaks corresponding to steps 1 and 2 could not be resolved under the experimental conditions. However, the observed $E_{p/2} - E_p$ value ($\sim 120 \text{ mV}$) is consistent with two closely separated reduction processes.

The complex $[\text{Ru}^{\text{III}}(\text{HEDTA})(\text{H}_2\text{O})]$ in the presence of hydrazine at high concentrations ($> 10 \text{ mM}$) gave two well-resolved cathodic peaks (I and II shown in Figure 6B), corresponding to polarographic wave steps 1 and 2, respectively, and one anodic peak. The cathodic peak I ($E_{p/2} - E_p$, 55 mV) shifted anodically with the increase in concentration of hydrazine but cathodically with the increase in scan speed. Moreover, the anodic counterpart to peak I was not seen at higher scan speeds or even after limiting the cathodic scan to the foot of peak II. From the above results and the results of polarography, it could be seen that the two-electron-reduced hydrazinium complexes (at peak I or step 1) are chemically unstable. Finally, peak II ($E_{p/2} - E_p$, 71 mV) and the anodic peak, which were less affected by the concentration of hydrazine or scan speed, are assigned to the Ru(III)/Ru(II) couple in the two-electron-reduced products of the hydrazinium complexes at peak I.

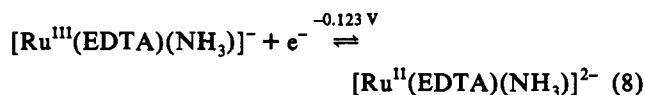
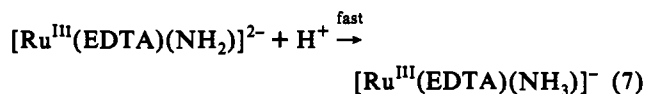
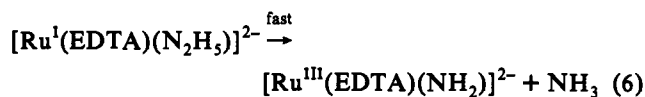
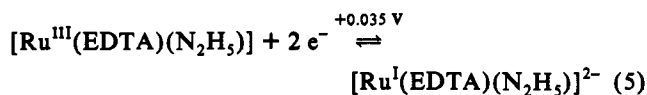
II. Constant Potential Electrolyses and Mechanism of Electroreduction of Hydrazinium Complexes. A solution of $[\text{Ru}^{\text{III}}(\text{HEDTA})(\text{H}_2\text{O})]$ (1 mM) at pH 3 in the presence of 1 equiv of hydrazine was reduced at a mercury pool cathode at -0.4 V vs SCE. The net charge consumed, equivalent to three electrons per metal, was the same as that of the isolated hydrazinium adduct but 3 times that for $[\text{Ru}^{\text{III}}(\text{HEDTA})(\text{H}_2\text{O})]$. Analysis of the reduced solution has confirmed the formation of 2 equiv of ammonia per mole of metal complex.

On the basis of the above results, the reduction of hydrazinium complex $[\text{Ru}^{\text{III}}(\text{EDTA})(\text{N}_2\text{H}_5)]$ (considered here for the sake of clarity and as it is the major species in solution at $\text{pH} > 2.3$) under steady-state conditions is represented as shown in Scheme 1

Scheme 1

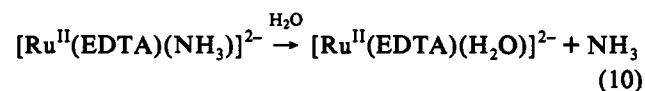
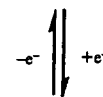
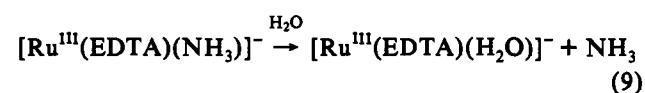


1 and eqs 5–8. A similar mechanism is applicable to the reduction of $[\text{Ru}^{\text{III}}(\text{HEDTA})(\text{N}_2\text{H}_5)]^+$.

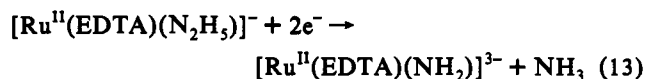
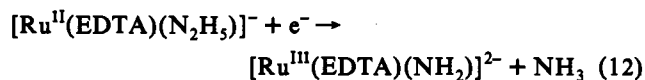
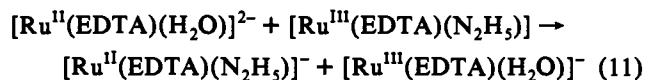


The reduced hydrazinium complex at $E_{1/2} \sim +0.035 \text{ V}$ in reaction 5 is unstable and decomposes irreversibly to 1 mol of NH_3 and the intermediate complex species $[\text{Ru}^{\text{III}}(\text{EDTA})(\text{NH}_2)]^{2-}$ (reaction 6). Species containing NH_x ($x = 1-3$) ligands have been postulated as the most plausible intermediates in the sequential reduction of N_2 to ammonia by the nitrogenase enzymes and in the reactions of certain dinitrogen complexes or their derivatives with protic or hydridic reagents.⁸ The amido complex $[\text{Ru}^{\text{III}}(\text{EDTA})(\text{NH}_2)]^{2-}$, since it is in acidic solution, immediately turns to an amine complex, $[\text{Ru}^{\text{III}}(\text{EDTA})(\text{NH}_3)]^-$, as in reaction 7. Then, one-electron reduction of $[\text{Ru}^{\text{III}}(\text{EDTA})(\text{NH}_3)]^-$, giving $[\text{Ru}^{\text{II}}(\text{EDTA})(\text{NH}_3)]^{2-}$ (reaction 8) at $E_{1/2} \approx -0.123 \text{ V}$, is assumed to be the following step.

Hydrolysis of $[\text{Ru}^{\text{III}}(\text{EDTA})(\text{NH}_3)]^-$ and $[\text{Ru}^{\text{II}}(\text{EDTA})(\text{NH}_3)]^{2-}$ produces another mole of NH_3 and their respective aquo complexes, as shown in reactions 9 and 10. The fact that



the $E_{1/2}$ of steps 1 and 2 had the least dependence on solution pH lends support to the protonation reaction 7 and the hydrolyses reactions 9 and 10. As the aquo complex $[\text{Ru}^{\text{II}}(\text{EDTA})(\text{H}_2\text{O})]^{2-}$ in reactions 9 and 10 can bind hydrazinium ion more effectively than the original complex, it can readily react with either $[\text{Ru}^{\text{III}}(\text{EDTA})(\text{N}_2\text{H}_5)]$ (reaction 11) or unbound hydrazinium ion in bulk, generating $[\text{Ru}^{\text{II}}(\text{EDTA})(\text{N}_2\text{H}_5)]^-$. The one- or two-electron reduction of this new species (reactions 12 and 13) at



the electrode could explain the catalytic nature of the enhanced current at $[\text{hydrazine}]/[\text{Ru}^{\text{III}}(\text{HEDTA})(\text{H}_2\text{O})] \leq 1$ and the disappearance of anodic response in CV at slow scan speeds.

III. Catalytic Reduction of Hydrazine to Ammonia. A series of controlled-potential electrolyses at -0.05 V were conducted on solutions containing excess $\text{N}_2\text{H}_5\text{HSO}_4$ in order to test the catalytic ability of $[\text{Ru}^{\text{III}}(\text{HEDTA})(\text{H}_2\text{O})]$ through its hydrazinium complexes for the reduction of hydrazine to ammonia. The net

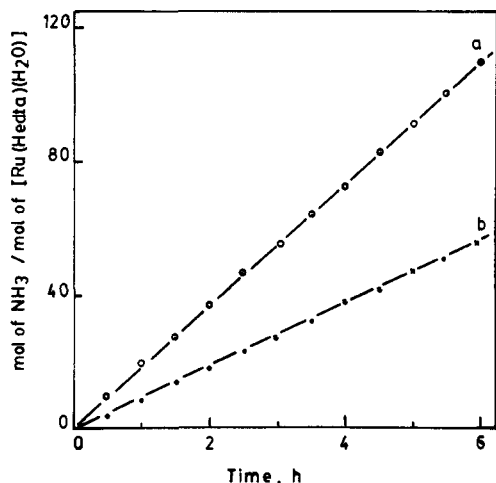
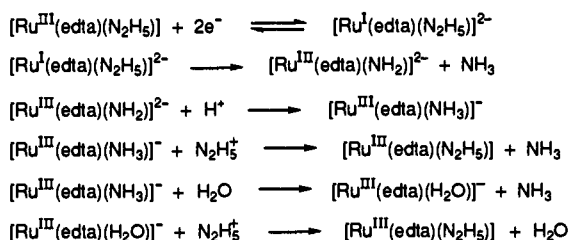


Figure 7. Plot of moles of NH_3 produced per mole of $[\text{Ru}^{\text{III}}(\text{HEDTA})(\text{H}_2\text{O})]$ vs time (h) at initial pH (a) 2.8 and (b) 1.9.

Scheme 2



reaction observed in all these experiments is constant reduction of hydrazine, justifying step 1 as a multielectron wave. The plots of moles of ammonia produced per mole of complex vs the electrolysis time (h) are linear (Figure 7) and consistent with the catalytic process as shown in Scheme 2. From slopes of these plots, the turnover numbers for the formation of moles of ammonia per mole of catalyst per hour are calculated to be 18.4 at pH 2.8 and 9.5 at pH 1.9 with 100% Coulombic efficiency. On comparison of this data with that reported earlier,^{27,28} the catalytic efficiency of the present complexes appears to be better.

When an additional amount of $\text{N}_2\text{H}_5\text{HSO}_4$ was added to the solution and electrolysis continued after adjusting the pH to the

initial value, the reduction of hydrazine took place with the same efficiency as in the earlier experiment, which shows the efficiency of the catalyst remained intact during the turnovers of hydrazine reduction. Further, there was no white precipitate of polyacrylonitrile observed on adding acrylonitrile⁴⁷ to the experimental solution, while electrolysis was going on. This ruled out the possibility of formation of free radicals in the reduction cycles.

Conclusions

The present study reveals that the complex $[\text{Ru}^{\text{III}}(\text{HEDTA})(\text{H}_2\text{O})]$ reacts with hydrazine to give $[\text{Ru}^{\text{III}}(\text{HEDTA})(\text{N}_2\text{H}_5)]^+$ and $[\text{Ru}^{\text{III}}(\text{EDTA})(\text{N}_2\text{H}_5)]$, which are stable at $\text{pH} < 4.5$. Both the complexes reduce at $+0.035$ V (Hg) vs Ag/AgCl to give $[\text{Ru}^{\text{I}}(\text{HEDTA})(\text{N}_2\text{H}_5)]^-$ and $[\text{Ru}^{\text{I}}(\text{EDTA})(\text{N}_2\text{H}_5)]^{2-}$. The reduced complexes rapidly decompose to $[\text{Ru}^{\text{III}}(\text{HEDTA})(\text{NH}_2)]^-$, $[\text{Ru}^{\text{III}}(\text{EDTA})(\text{NH}_2)]^{2-}$, and 1 mol of NH_3 via heterolytic cleavage of the N–N bond following the transfer of two electrons from Ru(I) to the bonded nitrogen. The amido complexes, on protonation, give the corresponding amine complexes $[\text{Ru}^{\text{III}}(\text{HEDTA})(\text{NH}_3)]$ and $[\text{Ru}^{\text{III}}(\text{EDTA})(\text{NH}_3)]^-$. Hydrolysis of $[\text{Ru}^{\text{III}}(\text{HEDTA})(\text{NH}_3)]$, $[\text{Ru}^{\text{III}}(\text{EDTA})(\text{NH}_3)]^-$, or their reduced products at -0.123 V (Hg) vs Ag/AgCl gives yet another mol of NH_3 with the regeneration of the aquo complex in its original oxidation state or one-electron-reduced form, respectively. The electroreduction of hydrazine catalyzed by the above hydrazinium complexes is achieved at very low reduction potential, -0.05 V (Hg) vs SCE, with 100% Coulombic efficiency. The present study thus shows the EDTA complexes of ruthenium as the first transition metal complexes that can activate and reduce the N–N bond of hydrazine to ammonia, with the help of a Hg electrode as an electron source in protic media.

Acknowledgment. G.R. gratefully acknowledges the reviewers of this paper and Prof. A. J. Bard, Editor of this journal, for a careful reading of the manuscript and for many critical comments and invaluable suggestions on many of the key issues. The author is also indebted to Prof. P. Natarajan, Director of this institute, for helpful comments and suggestions. Finally, G.R. wishes to thank Dr. Mohan Bhadbhade for help during the preparation of this paper.

(47) Gangopadhyay, S.; Ali, M.; Banerjee, P. *J. Chem. Soc., Perkin Trans. 2* 1992, 725.